# Some Problems in Stability of Heterogeneous Aeolotropic Cylindrical Shells under Combined Loading

B. P. C. Ho*
*Allis Chalmers Manufacturing Company, Milwaukee, Wis.*

AND

S. CHENG†
*University of Wisconsin, Madison, Wis.*

**Methods are described for the application of the results obtained in a previous paper. Several numerical problems have been computed, and results are presented in the form of curves. Solutions of problems in which all the boundary conditions are satisfied are compared with the solutions of the same problems in which the boundary conditions are satisfied only partially. These comparisons reveal the effect of the boundary conditions on the buckling load.**

## Nomenclature

| | | |
|---|---|---|
| $a$ | = | radius to middle surface of shell |
| $A,\bar{A},B,\bar{B},$ $C,\bar{C},D,\bar{D}$ | = | elastic coefficients |
| $e,\bar{e}$ | = | strain components |
| $E$ | = | Young's modulus |
| $G$ | = | shear modulus |
| $h$ | = | thickness of cylindrical shell |
| $k$ | = | buckling coefficient |
| $L$ | = | length of cylinder |
| $m$ | = | number of half-waves in axial direction |
| $M$ | = | resultant moment per unit length |
| $n$ | = | number of waves in circumferential direction |
| $N$ | = | resultant force per unit length |
| $P$ | = | external radial pressure |
| $p$ | = | external axial compression per unit length |
| $q$ | = | load parameter |
| $T$ | = | external torsional force per unit length |
| $u$ | = | axial displacement of middle surface |
| $v$ | = | circumferential displacement of middle surface |
| $w$ | = | radial displacement of middle surface |
| $x$ | = | axial coordinate of middle surface |
| $z$ | = | radial coordinate of middle surface |
| $\theta$ | = | circumferential coordinate of middle surface |
| $\lambda$ | = | dimensionless parameter |
| $\nu$ | = | Poisson's ratio |
| $\sigma,\bar{\sigma}$ | = | stress components |
| $\xi,\eta$ | = | major and minor elastic axes of orthotropic material parallel to $x$-$\theta$ plane |
| $\phi$ | = | angle between $x$ axis and $\xi$ axis |
| $\alpha$ | = | $h^2/12a^2$ |

## Introduction

METHODS are described for the application of the results derived in a previous paper.[1] In order to check the available test data,[5, 8, 12] numerical calculations are presented in the form of curves for these cases: 1) plywood of three equal layers with face grain directions 0°, 45°, 90° under the external radial load or under the torsion combined with radial load; and 2) isotropic material under the external radial load or under the torsion.

The boundary conditions for the foregoing cases are both ends of the cylinder hinged or both ends of the cylinder clamped. The numerical results of this paper check satisfactorily with the test results from the available literature.[5, 8, 12]

Since the present work concerns the application of the results derived in Ref. 1, reference for equations and other information should be made to that paper.‡

## Applications

In practical applications, orthotropic materials like plywood,[3] reinforced structure,[2] or glass-reinforced plastic[4] are used widely. The stress-strain relations of this kind of material referring to its own mutually perpendicular axes of elastic symmetry ($\bar{x}_1,\bar{x}_2,\bar{x}_3$) can be represented by[9]

$$\begin{pmatrix} \bar{\sigma}_{11} \\ \bar{\sigma}_{22} \\ \bar{\sigma}_{33} \\ \bar{\sigma}_{23} \\ \bar{\sigma}_{31} \\ \bar{\sigma}_{12} \end{pmatrix} = \begin{pmatrix} \bar{C}_{11}{}^{11} & \bar{C}_{22}{}^{11} & \bar{C}_{33}{}^{11} & 0 & 0 & 0 \\ \bar{C}_{22}{}^{11} & \bar{C}_{22}{}^{22} & \bar{C}_{33}{}^{22} & 0 & 0 & 0 \\ \bar{C}_{33}{}^{11} & \bar{C}_{33}{}^{22} & \bar{C}_{33}{}^{33} & 0 & 0 & 0 \\ 0 & 0 & 0 & \bar{C}_{23}{}^{23} & 0 & 0 \\ 0 & 0 & 0 & 0 & \bar{C}_{31}{}^{31} & 0 \\ 0 & 0 & 0 & 0 & 0 & \bar{C}_{12}{}^{12} \end{pmatrix} \begin{pmatrix} \bar{e}_{11} \\ \bar{e}_{22} \\ \bar{e}_{33} \\ \bar{e}_{23} \\ \bar{e}_{31} \\ \bar{e}_{12} \end{pmatrix} \quad (1)$$

where $\bar{C}_{mn}{}^{ij}$'s are elastic coefficients. Let $(x_1,x_2,x_3)$ be reference rectangular coordinates, and let $x_3$ coincide with $\bar{x}_3$. If the angle between the $\bar{x}_1$ axis and the $x_1$ axis is $\phi$, then the stress-strain relations referring to the reference coordinates $(x_1,x_2,x_3)$ become[7, 10]

$$\sigma_{ij} = C_{mn}{}^{ij} e_{mn} \quad (2)$$

$$C_{mn}{}^{ij} = l_{ip} l_{jq} l_{mr} l_{ns} \bar{C}_{rs}{}^{pq} \quad (3)$$

where $i,j,m,n,p,q,r,s = 1,2,3$, and $l_{ip}$, $l_{iq}$, $l_{mr}$, and $l_{ns}$ are direction cosines. For thin shells with the following indice transformation:

$$11 = 1 \qquad 22 = 2 \qquad 12, 21 = 6 \quad (4)$$

one has

$$\begin{aligned} C_{11} &= \bar{C}_{11}\cos^4\phi + \bar{C}_{22}\sin^4\phi + (\tfrac{1}{2}\bar{C}_{12} + \bar{C}_{66})\sin^2 2\phi \\ C_{12} &= \tfrac{1}{4}(\bar{C}_{11} + \bar{C}_{22} - 4\bar{C}_{66})\sin^2 2\phi + \bar{C}_{12}(\cos^4\phi + \sin^4\phi) \\ C_{16} &= \tfrac{1}{2}(\bar{C}_{11}\cos^2\phi - \bar{C}_{22}\sin^2\phi)\sin 2\phi - \tfrac{1}{4}(\bar{C}_{12} + 2\bar{C}_{66})\sin 4\phi \\ C_{22} &= \bar{C}_{11}\sin^4\phi + \bar{C}_{22}\cos^4\phi + (\tfrac{1}{2}\bar{C}_{12} + \bar{C}_{66})\sin^2 2\phi \end{aligned} \quad (5)$$

Received by IAS August 13, 1962; revision received January 24, 1963.

* Research Engineer, Research Division.

† Assistant Professor, Department of Mechanics and Mathematics Research Center.

‡ It should be noted that, in Figs. 4 and 10–13, the curves marked with $c^*$ are obtained from Eq. (19) of Ref. 1 without taking the boundary conditions into consideration. Similarly, the buckling coefficients $k^*$ in Fig. 9 are obtained from Eq. (19) of Ref. 1 without considering the boundary conditions.

$$C_{26} = \tfrac{1}{2}(\bar{C}_{11}\sin^2\phi - \bar{C}_{22}\cos^2\phi)\sin 2\phi + \tfrac{1}{4}(\bar{C}_{12} + 2\bar{C}_{66})\sin 4\phi$$

$$C_{66} = \tfrac{1}{4}(\bar{C}_{11} - 2\bar{C}_{12} + \bar{C}_{22})\sin^2 2\phi + \bar{C}_{66}\cos^2 2\phi$$

Referring to Fig. 1, the foregoing coordinates for tensor study can be related to the conventional coordinates as

$$x_1 = x \qquad x_2 = a\theta \qquad x_3 = z$$

$$\bar{x}_1 = \xi \qquad \bar{x}_2 = \eta \qquad \bar{x}_3 = \zeta$$

Usually, the following material properties are given or can be found from testing:

$E_\xi$ = Young's modulus along the major elastic axis of symmetry $\xi$

$E_\eta$ = Young's modulus along the minor elastic axis of symmetry $\eta$

$G$ = shear modulus in the $\xi\eta$ plane

$\nu_{\xi\eta},\nu_{\eta\xi}$ = Poisson's ratio, e.g., $\nu_{\xi\eta}$ is the ratio of the $\eta$ direction contraction to the $\xi$ direction extension associated with a $\xi$ direction tension

The relations between $\bar{C}_{ij}$ and $E_\xi,E_\eta,G,\nu_{\xi\eta},\nu_{\eta\xi}$ are[3]

$$\begin{aligned} \bar{C}_{11} &= E_\xi/\beta \qquad \bar{C}_{22} = E_\eta/\beta \\ \bar{C}_{12} &= E_\xi\nu_{\eta\xi}/\beta = E_\eta\nu_{\xi\eta}/\beta \\ \bar{C}_{66} &= G \qquad \beta = 1 - \nu_{\xi\eta}\nu_{\eta\xi} \end{aligned} \tag{6}$$

With Eqs. (5) and (6) available, the coefficients $A_{ij}$, $B_{ij}$, and $D_{ij}$ can be determined from Eqs. (10) of Ref. 1 for any

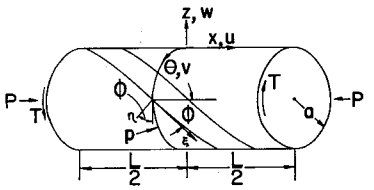


**Fig. 1 Orientation of axes in the middle surface of cylindrical shell**

orientation or inclination angle $\phi$ and any number of layers, provided the total thickness of the shell does not violate the thin shell theory.

The computer program can be divided into the following parts:

1) Calculation of the coefficients $\bar{A}_{ij}$, $\bar{B}_{ij}$, and $\bar{D}_{ij}$ (see Ref. 1) from the given geometric dimensions and physical properties using Eqs. (6, 5, 10, and 13) of Ref. 1.

2) Determination of critical load parameter $q_i$ and circumferential wave number $n$ from Eq. (19) of Ref. 1 with the load parameters $q_j$ and $q_k$ assumed to be given, where $i,j,k = 1,2,3$ and $i \neq j \neq k$.

3) Determination of the eight roots of $\lambda$ from the expanded polynomial of Eq. (18) of Ref. 1 by the Bairstow method.[11]

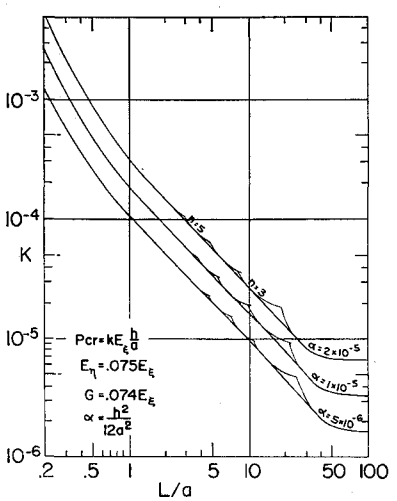


**Fig. 2 Buckling coefficient for plywood cylindrical shells under external radial pressure; plywood of three plies of equal thickness, grain direction of face plies axial; both ends hinged**

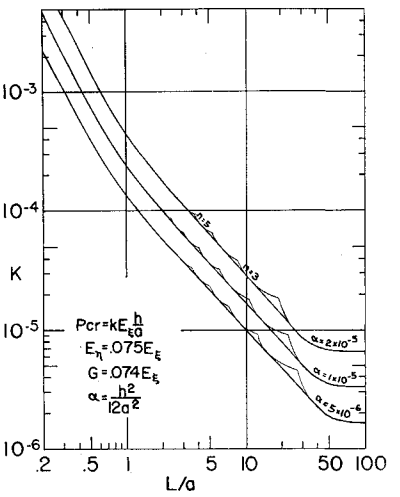


**Fig. 3 Buckling coefficient for plywood cylindrical shells under external radial pressure; plywood of three plies of equal thickness, grain direction of face plies axial; both ends clamped**

4) Determination of length $L$ from the zero determinant of the boundary characteristic, Eqs. (45) of Ref. 1, by the conventional elimination method.

For plywood with the physical properties[8, 3]

$$E_\eta/E_\xi = 0.075 \qquad G/E_\xi = 0.074$$
$$\nu_{\xi\eta} = 0.373 \qquad \nu_{\eta\xi} = 0.028$$

some sample calculations were run by the CDC 1604 computer for the following cases:

1) Load: radial pressure only.

2) Configuration: three layers of equal thickness with orientations: 1) 0°, 90°, 180°; 2) 45°, 135°, 225°; and 3) 90°, 180°, 270°.

3) Boundary conditions: 1) both ends hinged: $w = 0$, $T_x = 0$, $N_x = 0$, and $M_x = 0$; and 2) both ends clamped: $w = 0$, $T_x = 0$, $N_x = 0$, and $w_{,x} = 0$.

The compiling time of the program is about 90 sec. The calculating time for each run (determination of $q_{cr}$, $n$, the eight roots of $\lambda$, and the $L/a$'s for hinged and clamped boundary conditions) takes about 6 sec. Because the computer has quite a low absolute value limit of the argument of the hyperbola cosine or hyperbola sine, a common factor of $\cosh(\lambda_i L/2a)_k$ may be factored out from each $k$ ($k = 1, 2, \ldots, 8$) column of the boundary characteristic, Eqs. (45) of Ref. 1, and set $\tanh(\arg) = \pm 1$ when $20 < \arg < -20$. The results are presented in Figs. 2–7.

Other cases also were run, such as the following:

1) Isotropic cylindrical shells under external radial pressure with boundary conditions similar to those in the previous cases (see Fig. 8).

2) Plywood cylindrical shells having similar configurations to previous ones under combined torsion and radial pressure with the following boundary conditions: 1) both ends

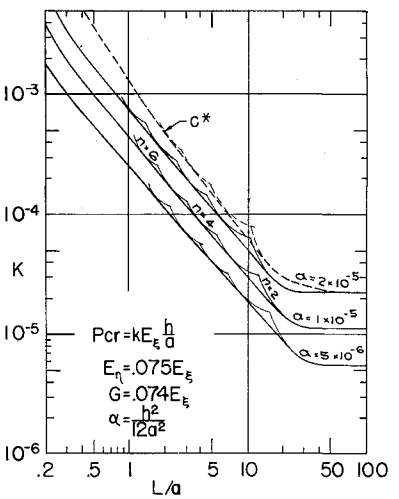


**Fig. 4 Buckling coefficient for plywood cylindrical shells under external radial pressure; plywood of three plies of equal thickness, grain direction of face plies 45° from axial axis; both ends hinged. $c^*$ is calculated from Eq. (19) of Ref. 1 without considering boundary conditions**

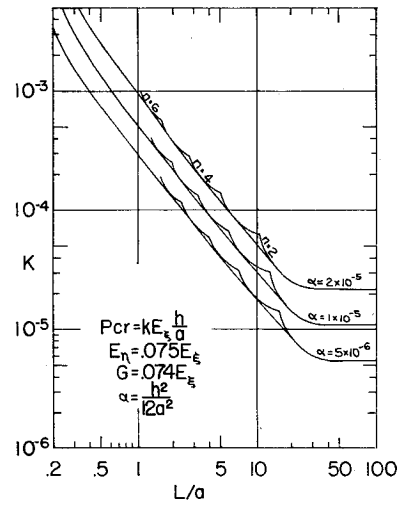


**Fig. 5 Buckling coefficient for plywood cylindrical shells under external radial pressure; plywood of three plies of equal thickness, grain direction of face plies 45° from axial axis; both ends clamped**

hinged: $w = 0$, $N_x + Tu_{,\theta}/a = 0$, $T_x = 0$, and $M_x = 0$; and 2) both ends clamped: $w = 0$, $N_x + Tu_{,\theta}/a = 0$, $T_x = 0$, and $w_{,x} = 0$. Physical properties are[12] $E\eta/E_\xi = 0.045$, $G/E_\xi = 0.056$, $\nu_{\xi\eta} = 0.434$, and $\nu_{\eta\xi} = 0.024$ (see Figs. 9–11).

3) Isotropic cylindrical shells under torsion with boundary conditions the same as in case 2 (see Fig. 12).

## Discussions

### A. Buckling of Cylindrical Shells under External Radial Pressure

As shown in Fig. 13, the effect of the boundary conditions on the buckling load for both ends clamped increases as the ratio $L/a$ decreases. The point at which this effect starts to be significant is different for different materials. The effect for both ends hinged is apparently zero for isotropic material and for plywood of face grain direction axial. For plywood of face grain direction 45° from axial axis, the effect of the boundary conditions on the buckling load is more significant. It is because the elastic coefficients $C_{16}$ and $C_{26}$ are not zero any more [see Eqs. (5)], as in the case of isotropic material or plywood of face grain direction axial or circumferential.

As was mentioned in Ref. 1, Flugge's Eq. (VII-10)[6] is a particular case of Eq. (18) of Ref. 1. Hence, the curve of $\alpha = 2 \times 10^{-5}$ with both ends hinged, as shown in Fig. 8, checks almost identically with Flugge's Fig. VII-15.[6]

Figures 38 and 39 of Ref. 8, based on Cheng's analysis,[3] also check well with Figs. 6 and 2 of this paper for infinite length. Jenkinsen et al.[8] compared their test results for plywood of face grain direction circumferential and axial with Cheng's theoretical values.[3] The average ratio of test $p_{cr}$ to theoretical $p_{cr}$ is about 0.85 for face grain direction circumferential and

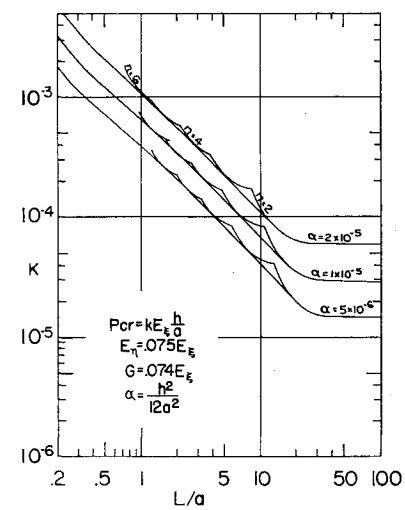


**Fig. 6 Buckling coefficient for plywood cylindrical shells under external radial pressure; plywood of three plies of equal thickness, grain direction of face plies circumferential; both ends hinged**

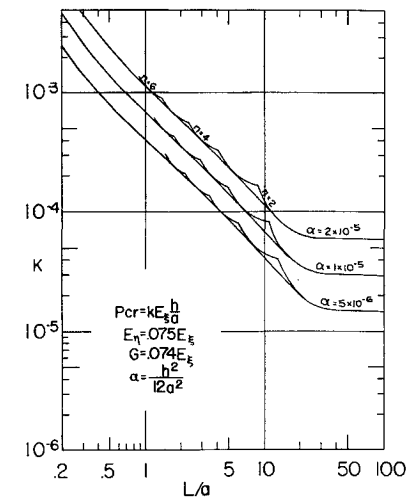


**Fig. 7 Buckling coefficient for plywood cylindrical shells under external radial pressure; plywood of three plies of equal thickness, grain direction of face plies circumferential; both ends clamped**

1.04 for face grain direction axial. There were 11 tests for the former case and 10 for the latter. All plywood cylindrical shells are of three plies of equal thickness. If a correction factor of 0.95 (from Fig. 13) is applied to the former case, then the average ratio of test $p_{cr}$ to theoretical $p_{cr}$ will rise from 0.85 to 0.90. Jenkinsen et al. also made 10 tests of the same plywood with face grain direction of the cylindrical shells to be 45° from the axial axis. However, they did not make comparisons for this case because the theoretical formula was not available. Based on the average dimensions and calculated Young's modulus in the ply grain direction, from Fig. 4, the average ratio of test $p_{cr}$ to theoretical $p_{cr}$ for three-ply plywood cylindrical shells with face grain direction 45° from axial axis is 4.80 to 5.65, or 0.85.

### B. Buckling of Cylindrical Shells under Combined Torsion and Radial Pressure

Figures 9–11 (for plywood cylindrical shells) show that boundary conditions do affect the buckling loads a great deal even if the ratio $L/a$ is quite large, for example, 50. The difference of the effects between the case of both ends hinged and the case of both ends clamped is not significant until the ratio $L/a$ becomes small. It is interesting to notice that the effect of radial pressure on the torsional buckling load becomes insignificant when the ratio $L/a$ is small, whether the radial pressure is external or internal. The small circles in Figs. 9–11 show that the theoretical results of this analysis agree well with those of March et al.[12] According to their report, the test results agree satisfactorily with the theoretical calculations. Hence, those test results also should check satisfactorily with the authors' theoretical calculations.

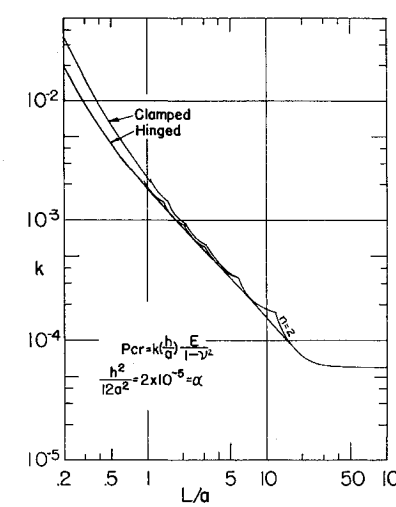


**Fig. 8 Buckling coefficient for isotropic cylindrical shells under external radial pressure**

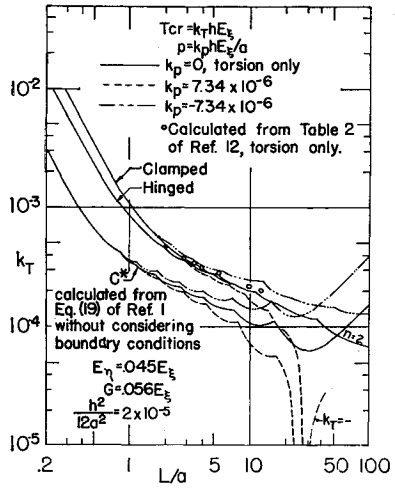


**Fig. 9 Buckling coefficient for plywood cylindrical shells under combined torsion and radial pressure; plywood of three plies of equal thickness, grain direction of face plies axial**

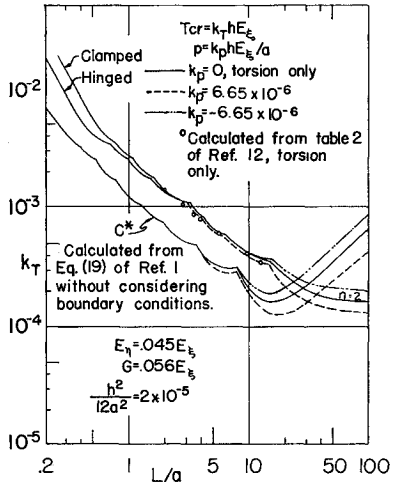


**Fig. 10 Buckling coefficient for plywood cylindrical shells under combined torsion and radial pressure; plywood of three plies of equal thickness, grain direction of face plies 45° from axial axis**

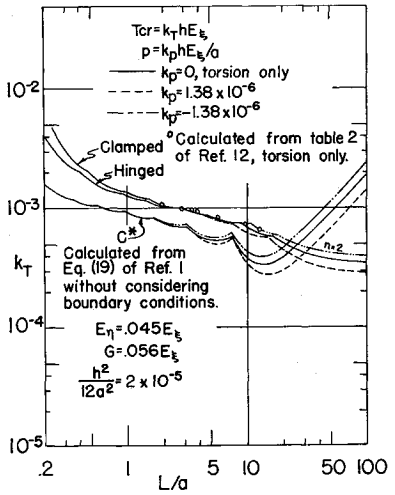


**Fig. 11 Buckling coefficient for plywood cylindrical shells under combined torsion and radial pressure; plywood of three plies of equal thickness, grain direction of face plies circumferential**

Figure 12 (for isotropic cylindrical shells under torsion only) shows that the authors' curves§ are lower than Donnell's.[5] They approach each other respectively when the parameter $(1 - \nu^2)^{1/2}L^2/(2ah)$ is small. Furthermore, the difference in the effects of the boundary conditions between the cases of both ends hinged and both ends clamped does not show as clearly in the authors' curves as it does in Donnell's when the parameter $(1 - \nu^2)^{1/2}L^2/(2ah)$ is greater than 50. This may be due to the oversimplification in Donnell's analysis.[5]

§ Other boundary conditions also were calculated, i.e., substituting $v = 0$ and $u = 0$ or $T_x = 0$ and $u = 0$ for $T_x = 0$ and $N_x + Tu_{,\theta}/a = 0$. The usual other two conditions, $w = 0$ and $M_x = 0$ or $w = 0$ and $w_{,x} = 0$, were not changed. No significant difference resulted.

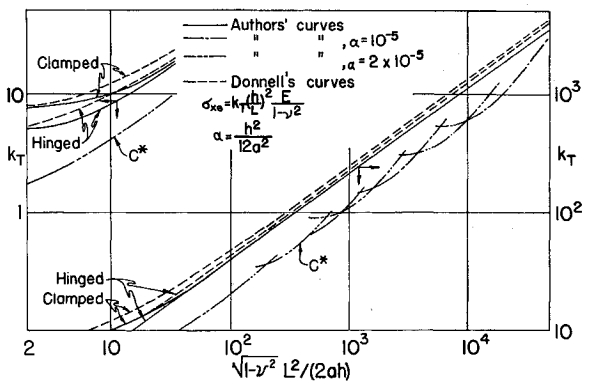


**Fig. 12 Buckling coefficient for isotropic cylindrical shells under torsion. $c^*$ is calculated from Eq. (19) of Ref. 1 without considering boundary conditions**

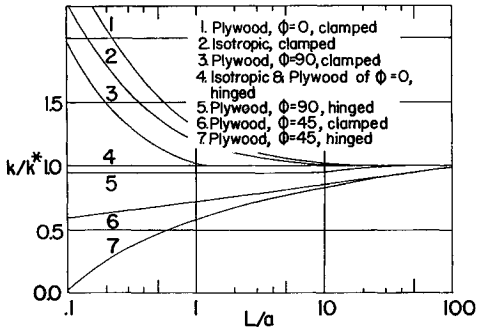


**Fig. 13 Correction factor, ratio of theoretical buckling coefficient to buckling coefficient $k^*$, for three-ply plywood and isotropic cylindrical shells under external radial pressure. $k^*$ is calculated from Eq. (19) of Ref. 1 without considering boundary conditions**

In Fig. 1 of Donnell's paper, most test points are below his theoretical curves. Hence, the authors' curves should check the test results better than Donnell's.

## Conclusions

This analysis not only determines the buckling of heterogeneous aeolotropic cylindrical shells under combined axial, radial, and torsional loads, but it also satisfies all four boundary conditions at each end of the cylinder. Most related theoretical derivations[3, 5, 6, 12] are particular cases of this analysis. Test results usually agree fairly well (except under axial compression) with their theoretical calculations. There is no doubt that those test results should agree equally well, or even better, with this analysis, because all four boundary conditions at each end of the cylinder are satisfied. The only limitation of this analysis is that the axial load should be limited to tension or small compression in combination with other loads.

## References

[1] Cheng, S. and Ho, B. P. C., "Stability of heterogeneous aeolotropic cylindrical shells under combined loading," AIAA J. **1**, 892–898 (1963).

[2] Beckner, H. and Gerard, G., "Elastic stability of orthotropic shells," J. Aerospace Sci. **29**, 505–512 (1962).

[3] Cheng, S., "Buckling of orthotropic or plywood cylindrical shells under external radial pressure," Forest Products Lab. Rept. PE-216 (1961).

[4] Cutler, V. C., "Bending analysis of directionally reinforced pipes," Univ. Wis., Ph.D. Dissertation (1960).

[5] Donnell, L. H., "Stability of thin-walled tubes under torsion," NACA Rept. 479, pp. 95–115 (1934).

[6] Flugge, W., *Stresses in Shells* (Springer-Verlag, Berlin, 1962).
[7] Green, A. and Zerne, W., *Theoretical Elasticity* (Oxford University Press, London, 1954).
[8] Jenkinsen, P. M., McAlister, R. H., Lutz, J. F., and Kuenzi, E. W., "Evaluation of plywood cylindrical shells subjected to external radial pressure," Forest Products Lab. Rept. PE-224 (October 1961).
[9] Sokolnikoff, I. S., *Mathematical Theory of Elasticity* (McGraw-Hill Book Co. Inc., New York, 1956).
[10] Sokolnikoff, I. S., *Tensor Analysis* (John Wiley and Sons Inc., New York, 1951).
[11] Stanton, R. G., *Numerical Methods for Science and Engineering* (Prentice-Hall Inc., Englewood Cliffs, N. J., 1961).
[12] March, H. W., Norris, C. B., Smith, C. B., and Kuenzi, E. W., "Buckling of thin-walled plywood cylinders in torsion," Forest Products Lab. Rept. 1529 (June 1945).

JULY 1963 AIAA JOURNAL VOL. 1, NO. 7

# Plastic Instability of Cylindrical Pressure Vessels of Finite Length

P. MANN-NACHBAR,* O. HOFFMAN,† AND W. E. JAHSMAN†

*Lockheed Missiles and Space Company, Sunnyvale, Calif.*

**A mathematical analysis is given for the plastic instability of an internally pressurized cylindrical shell of finite length. The ends of the shell are free to rotate and to translate axially but are restrained from radial motion. Tresca's yield condition and the associated flow rule are used, and the shell material obeys Ludwik's power law, $\sigma_e = C(\epsilon_e)^n$, where $\sigma_e$ and $\epsilon_e$ are the effective stress and strain, and $C$ and $n$ are material constants. When the deformed shape of the meridian of the pressurized shell can be represented by a parabola, the instability pressure increases from the known value for long shells to approximately twice that value for short shells. The bulk of the increase in the instability pressure occurs for the shells with length less than diameter. For fixed shell length, the instability pressure increases with increasing values of the strain-hardening exponent $n$.**

## Introduction

UNTIL recently, studies of plastic tension instability have dealt with rather simple structural elements such as rods, plates, and infinite cylinders.[1] In particular, the effects of end constraints have not been considered. Within the past two years, however, two independent reports have appeared which deal with the strengthening effect of end constraints on the plastic instability of internally pressurized cylinders of finite length, the ends of which are restrained against radial motion.[2, 3] These reports show that, as the length-to-diameter ratio of the cylinder decreases toward unity, the instability pressure, i.e., the local maximum of the pressure function $p = p(\epsilon_e)$, increases slightly, usually by less than 10%. Below length-to-diameter ratios of unity, these solutions cease to be valid because the total strain (or deformation) theory of plasticity is used in the analyses. As is well known, this theory applies only for nearly constant stress ratios, and it is shown in Ref. 2 that this condition generally requires length-to-diameter ratios greater than unity.

In the present paper, the incremental (or flow) theory of plasticity is used, and no limitations on length-to-diameter ratios appear. A complete range of dependence of the instability pressure on length-to-diameter ratios ranging from zero to infinity is developed. For some ranges of length-to-diameter ratios, two instability pressures (i.e., two local pressure maxima) are found, with the larger instability pressure occurring at rather large deformations. If the cylinder material has limited ductility, the smaller instability pressure may govern; otherwise, failure will occur at the larger instability pressure. Final results give both instability pressures, so that the range of possible failure pressures is available. It is found that the ends of the cylinder have a pronounced strengthening effect when the length is less than the diameter. This trend also is observable in published experimental data.[4]

Presented at the IAS 31st Annual Meeting, New York, January 20–23, 1963; revision received May 10, 1963.

* Staff Scientist, Mechanical and Mathematical Sciences Laboratory.
† Senior Staff Scientist, Mechanical and Mathematical Sciences Laboratory.

## Basic Equations

A cylindrical pressure vessel of initial radius $R$ and length $2L$ has end supports that permit meridional rotation and axial extension but prevent radial motion. Under pressurization, the vessel will "barrel out" and change length as shown in Fig. 1. Equilibrium of the deformed cylinder is governed by the membrane relations

$$\sigma_\phi = pr_2/2h \tag{1}$$

$$\sigma_\theta = (pr_2/2h)[2 - (r_2/r_1)] \tag{2}$$

where $\sigma_\phi$ and $\sigma^\theta$ are the meridional and circumferential membrane stresses,‡ $p$ is the internal pressure, $h$ is the instantaneous wall thickness, and $r_1$ and $r_2$ are the principal radii of curvature shown in Fig. 2. The radius $r_1$ lies in the meridional plane and is related to the instantaneous distance from the shell to the axis $r$ by

$$r_1 = -(1 + r'^2)^{3/2}/r'' \tag{3}$$

whereas the radius $r_2$ lies in the plane perpendicular to the

‡ As usual, the transverse normal stress $\sigma_r$ is neglected in comparison with $\sigma_\phi$ and $\sigma_\theta$.